SINGULAR STRESS FIELDS OF ANISOTROPIC BIMATERIAL WEDGES WITH IMPERFECT INTERFACES

Anil C. Wijeyewickrema [*] **Somsak Leungvichcharoen** [**]

Department of Civil Engineering
Tokyo Institute of Technology
Tokyo 152-8552, Japan

Piya Poonsawat [***]

School of Civil Engineering
Rangsit University
Pathumthani 12000, Thailand

ABSTRACT

The effect of an imperfect interface on the stress singularity of anisotropic bimaterial wedges subjected to traction free boundary conditions are investigated. The interfacial tractions are assumed to be continuous, directly proportional to the displacement jumps and inversely proportional to the radial coordinate. The characteristic equation for the order of singularity is obtained and numerical results are given for the angle-ply bimaterial composite wedge.

Keywords : Anisotropic elasticity, Bimaterial composite wedge, Imperfect interface, Singularities.

1. INTRODUCTION

The study of singular stress fields in an anisotropic elastic wedge was initiated by Benthem [1]. Subsequent related studies of an anisotropic elastic wedge are referenced in Ma and Hour [2] and Chue and Liu [3]. Free-edge singular stresses of layered anisotropic composite wedges under extension have been studied by Wang and Choi [4] and Zwiers, *et al*. [5]. One of the first studies of bimaterial anisotropic elastic composite wedges with arbitrary wedge angles is the work of Delale [6], who investigated the stress singularities of an anisotropic bimaterial wedge.

Lin and Sung [7] considered the stress singularities of a bimaterial anisotropic elastic composite wedge and provided comprehensive results for the inplane problem of aligned orthotropic composites. More recently Poonsawat, *et al*. [8] have considered both angle-ply and monoclinic bimaterial wedges with fully bonded and frictional interfaces. While Lin and Sung [7] and Poonsawat, *et al*. [8] have used the Stroh formalism in their work, Chue and co-workers [9~11] have used a Lekhnitskii formulation when considering a bimaterial anisotropic composite wedge.

In the present analysis anisotropic elastic bimaterial wedges which are not perfectly bonded at the interface and where the wedge faces are traction free, are considered. Here the interfacial tractions are assumed to be continuous, directly proportional to the displacement jumps and inversely proportional to the radial coordinate. This model of the imperfect interface is similar to that adopted by Mishuris [12~14] when considering a crack normal to the interface of two isotropic materials.

In Section 2, using the Stroh formalism, the relevant expressions for displacements and stresses for two-dimensional problems are given. The stress singularity analysis of an anisotropic wedge is presented in Section 3 and the anisotropic bimaterial composite wedge with an imperfect interface is considered in Section 4. Numerical results for a fiber reinforced composite wedge are presented in Section 5.

2. BASIC EQUATIONS OF ANISOTROPIC ELASTIC MATERIALS

The displacement field for two-dimensional problems where all physical quantities depend only on the x_1 and x_2 coordinates, can be written as

$$u_i(x_1, x_2) = a_i\, f(x_1 + p x_2) \qquad i = 1, 2, 3 \qquad (1)$$

where $f(z)$ is an analytic function of the complex

* Associate Professor ** Graduate student *** Assistant Professor

variable $z = x_1 + px_2$ (Stroh [15]). It can be shown that the constant p is determined from the sextic equation

$$| C_{i1k1} + p(C_{i1k2} + C_{i2k1}) + p^2 C_{i2k2} | = 0 \qquad (2a)$$

and the constants a_i are determined from

$$[C_{i1k1} + p(C_{i1k2} + C_{i2k1}) + p^2 C_{i2k2}]\, a_k = 0 \qquad (2b)$$

where $C_{ijkl} = C_{jikl} = C_{ijlk} = C_{klij}$ are the elastic stiffnesses and repeated Latin indices imply summation. Since Eshelby, *et al*. [16] have shown that the roots of Eq. (2a) cannot be real, when all six roots are assumed to be distinct, the three different pairs of complex conjugates are denoted by p_α and $\overline{p}_\alpha$ (α = 1, 2, 3), where the imaginary part of p_α is taken to be positive and an overbar represents the complex conjugate. The value of a_i corresponding to p_α and $\overline{p}_\alpha$ are denoted by $a_{i\alpha}$ and $\overline{a}_{i\alpha}$.

The expressions for the displacement and stress fields can be obtained in the polar coordinate system (r, θ) as

$$u_i(r, \theta) = \sum_{\alpha=1}^{3} [a_{i\alpha} f_\alpha(r\zeta_\alpha) + \overline{a}_{i\alpha} g_\alpha(r\overline{\zeta}_\alpha)] \qquad (3)$$

$$\sigma_{i1}(r, \theta) = -\sum_{\alpha=1}^{3} [p_\alpha b_{i\alpha} f'_\alpha(r\zeta_\alpha) + \overline{p}_\alpha \overline{b}_{i\alpha} g'_\alpha(r\overline{\zeta}_\alpha)] \qquad (4a)$$

$$\sigma_{i2}(r, \theta) = \sum_{\alpha=1}^{3} [b_{i\alpha} f'_\alpha(r\zeta_\alpha) + \overline{b}_{i\alpha} g'_\alpha(r\overline{\zeta}_\alpha)] \qquad (4b)$$

where

$$\zeta_\alpha \equiv \zeta_\alpha(\theta) = \cos\theta + p_\alpha \sin\theta$$
$$b_{i\alpha} = -\frac{1}{p_\alpha}(C_{i1k1} + p_\alpha C_{i1k2})\, a_{k\alpha} \qquad (5)$$

The traction on a radial plane with a unit outward normal vector with components $\hat{n}_j \equiv (-\sin\theta, \cos\theta, 0)$ can be obtained as

$$t_i(r, \theta) = \sigma_{ij}\, \hat{n}_j = -\sigma_{i1} \sin\theta + \sigma_{i2} \cos\theta$$
$$= \sum_{\alpha=1}^{3} [\zeta_\alpha b_{i\alpha} f'_\alpha(r\zeta_\alpha) + \overline{\zeta}_\alpha \overline{b}_{i\alpha} g'_\alpha(r\overline{\zeta}_\alpha)] \qquad (6)$$

More details of the equations given in this section can be found in Poonsawat, *et al*. [8].

3. SINGULAR STRESS ANALYSIS OF AN ANISOTROPIC WEDGE

Following the work of Ting and Chou [17], let

$$f_\alpha(r\zeta_\alpha) = (r\zeta_\alpha)^{1-k}\, m_\alpha / (1-k)$$
$$g_\alpha(r\zeta_\alpha) = (r\overline{\zeta}_\alpha)^{1-k}\, n_\alpha / (1-k) \qquad (7)$$

where m_α and n_α are arbitrary constants so that $\sigma_{ij} = r^{-k} F_{ij}(\theta)$, where k is the order of singularity and r is the distance from the wedge apex. The value of k can be either real or complex. To ensure that the strain energy is bounded everywhere including the region where $r \to 0$, the order of singularity of interest is in the range $0 < \mathrm{Re}(k) < 1$. Hence, Eqs. (3), (4a), (4b) and (6) can be rewritten as

$$\mathbf{u}(r, \theta) = \frac{r^{1-k}}{1-k}(\mathbf{A} < \zeta_*^{1-k} > \mathbf{m} + \overline{\mathbf{A}} < \overline{\zeta}_*^{1-k} > \mathbf{n}) \qquad (8)$$

$$\boldsymbol{\sigma}_1(r, \theta) = -r^{-k}(\mathbf{B} < p_*\, \zeta_*^{-k} > \mathbf{m} + \overline{\mathbf{B}} < \overline{p}_*\, \overline{\zeta}_*^{-k} > \mathbf{n}) \qquad (9a)$$

$$\boldsymbol{\sigma}_2(r, \theta) = r^{-k}(\mathbf{B} < \zeta_*^{-k} > \mathbf{m} + \overline{\mathbf{B}} < \overline{\zeta}_*^{-k} > \mathbf{n}) \qquad (9b)$$

$$\mathbf{t}(r, \theta) = r^{-k}(\mathbf{B} < \zeta_*^{1-k} > \mathbf{m} + \overline{\mathbf{B}} < \overline{\zeta}_*^{1-k} > \mathbf{n}) \qquad (10)$$

where

$$\mathbf{u} = \{u_i\}, \quad \boldsymbol{\sigma}_1 = \{\sigma_{i1}\}, \quad \boldsymbol{\sigma}_2 = \{\sigma_{i2}\}, \quad \mathbf{t} = \{t_i\}$$
$$\mathbf{A} = [a_{i\alpha}], \quad \mathbf{B} = [b_{i\alpha}], \quad \mathbf{m} = \{m_\alpha\}, \quad \mathbf{n} = \{n_\alpha\} \qquad (11)$$

and the angle brackets denote diagonal matrices, i.e.,

$$< \zeta_*^{-k} > = \begin{bmatrix} \zeta_1^{-k} & 0 & 0 \\ 0 & \zeta_2^{-k} & 0 \\ 0 & 0 & \zeta_3^{-k} \end{bmatrix}$$
$$< p_*\, \zeta_*^{-k} > = \begin{bmatrix} p_1 \zeta_1^{-k} & 0 & 0 \\ 0 & p_2 \zeta_2^{-k} & 0 \\ 0 & 0 & p_3 \zeta_3^{-k} \end{bmatrix} \qquad (12)$$

Here, the unknown vectors $\mathbf{m}$ and $\mathbf{n}$ can be determined from given boundary conditions. Since the matrices $\mathbf{A}$ and $\mathbf{B}$ are not singular when p_α are distinct (Eshelby, *et al*. [16]), for convenience, in the formulation $\mathbf{m}$ and $\mathbf{n}$ can be replaced by $\mathbf{B}^{-1}\mathbf{m}$ and $\overline{\mathbf{B}}^{-1}\mathbf{n}$, respectively. Then it follows from Eqs. (8) ~ (10) that

$$\mathbf{u}(r, \theta) = -i\frac{r^{1-k}}{1-k}(\mathbf{M}^{-1}\mathbf{B} < \zeta_*^{1-k} > \mathbf{B}^{-1}\mathbf{m} - \overline{\mathbf{M}}^{-1}\overline{\mathbf{B}} < \overline{\zeta}_*^{1-k} > \overline{\mathbf{B}}^{-1}\mathbf{n}) \qquad (13)$$

$$\boldsymbol{\sigma}_1(r, \theta) = -r^{-k}(\mathbf{B} < p_*\, \zeta_*^{-k} > \mathbf{B}^{-1}\mathbf{m} + \overline{\mathbf{B}} < \overline{p}_*\, \overline{\zeta}_*^{-k} > \overline{\mathbf{B}}^{-1}\mathbf{n}) \qquad (14a)$$

$$\boldsymbol{\sigma}_2(r, \theta) = r^{-k}(\mathbf{B} < \zeta_*^{-k} > \mathbf{B}^{-1}\mathbf{m} + \overline{\mathbf{B}} < \overline{\zeta}_*^{-k} > \overline{\mathbf{B}}^{-1}\mathbf{n}) \qquad (14b)$$

$$\mathbf{t}(r, \theta) = r^{-k}(\mathbf{B} < \zeta_*^{1-k} > \mathbf{B}^{-1}\mathbf{m} + \overline{\mathbf{B}} < \overline{\zeta}_*^{1-k} > \overline{\mathbf{B}}^{-1}\mathbf{n}) \qquad (15)$$

The equations corresponding to the situation when p_α are not distinct were studied by Ting and Chou [17]. In Eq. (13), the impedance matrix $\mathbf{M}$ and its inverse are defined by

$$\mathbf{M} = -i\, \mathbf{B}\mathbf{A}^{-1}, \qquad \mathbf{M}^{-1} = i\, \mathbf{A}\mathbf{B}^{-1} \qquad (16)$$

4. AN ANISOTROPIC BIMATERIAL WEDGE WITH AN IMPERFECT INTERFACE

The anisotropic bimaterial composite wedge which consists of two wedges with the interface along the x_1-x_3 plane, is shown in Fig. 1. The upper wedge occupies the domain $0 \le \theta \le \theta_1$, whereas the lower wedge occupies the domain $-\theta_2 \le \theta \le 0$. Superscripts or subscripts (1) and (2) are used to denote the quantities associated with the upper wedge and the lower wedge, respectively.

The traction-free boundary conditions at the wedge faces are

$$t_i^{(1)}(r, \theta_1) = 0\,, \quad t_i^{(2)}(r, -\theta_2) = 0 \qquad i = 1, 2, 3 \quad (17)$$

Making use of Eq. (17), the expressions for displacements and tractions in Eqs. (13) and (15) can be written for different regions as follows:

For the upper wedge 1, i.e., $0 \le \theta \le \theta_1$:

$$\mathbf{u}^{(1)}(r, \theta) = -i\frac{r^{1-k}}{1-k}(\mathbf{M}_{(1)}^{-1}\,\mathbf{\Gamma}_{(1)}(\theta, k)\,\mathbf{\Omega}_{(1)}(k) + \overline{\mathbf{M}}_{(1)}^{-1}\,\overline{\mathbf{\Gamma}}_{(1)}(\theta, k)\,\overline{\mathbf{\Omega}}_{(1)}(k))\,\mathbf{m}^{(1)} \quad (18a)$$

$$\mathbf{t}^{(1)}(r, \theta) = r^{-k}(\mathbf{\Gamma}_{(1)}(\theta, k)\,\mathbf{\Omega}_{(1)}(k) - \overline{\mathbf{\Gamma}}_{(1)}(\theta, k)\,\overline{\mathbf{\Omega}}_{(1)}(k))\,\mathbf{m}^{(1)} \quad (18b)$$

For the lower wedge 2, i.e., $-\theta_2 \le \theta \le 0$:

$$\mathbf{u}^{(2)}(r, \theta) = -i\frac{r^{1-k}}{1-k}(\mathbf{M}_{(2)}^{-1}\,\mathbf{\Gamma}_{(2)}(\theta, k)\,\mathbf{\Omega}_{(2)}(k) + \overline{\mathbf{M}}_{(2)}^{-1}\,\overline{\mathbf{\Gamma}}_{(2)}(\theta, k)\,\overline{\mathbf{\Omega}}_{(2)}(k))\,\mathbf{m}^{(2)} \quad (19a)$$

$$\mathbf{t}^{(2)}(r, \theta) = r^{-k}(\mathbf{\Gamma}_{(2)}(\theta, k)\,\mathbf{\Omega}_{(2)}(k) - \overline{\mathbf{\Gamma}}_{(2)}(\theta, k)\,\overline{\mathbf{\Omega}}_{(2)}(k))\,\mathbf{m}^{(2)} \quad (19b)$$

where

$$\mathbf{\Gamma}_{(N)}(\theta, k) = \mathbf{B}_{(N)}\left\langle \zeta_{*(N)}^{1-k}(\theta)\right\rangle \mathbf{B}_{(N)}^{-1} \qquad N = 1, 2 \quad (20a)$$

$$\mathbf{\Omega}_{(1)}(k) = (\Gamma_{(1)}(\theta_1, k))^{-1} \quad (20b)$$

$$\mathbf{\Omega}_{(2)}(k) = (\Gamma_{(2)}(-\theta_2, k))^{-1} \quad (20c)$$

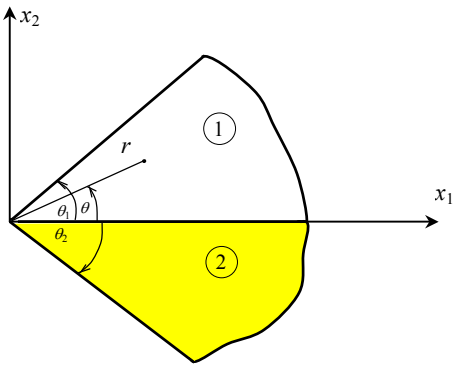

Fig. 1 A bimaterial anisotropic composite wedge

At the interface the tractions are assumed to be continuous, and directly proportional to the displacement jumps and also inversely proportional to the radial coordinate (Mishuris [12~14]),

$$t_i^{(1)}(r, 0) = t_i^{(2)}(r, 0)\,, \quad t_i^{(1)}(r, 0) = \frac{\lambda_{ij}}{r}[u_j^{(1)}(r, 0) - u_j^{(2)}(r, 0)] \qquad i, j = 1, 2, 3 \quad (21)$$

where λ_{ij} are the interfacial stiffness parameters. Substituting Eqs. (18a), (18b) and (19a), (19b) into Eq. (21) results in

$$(\mathbf{\Omega}_{(1)}(k) - \overline{\mathbf{\Omega}}_{(1)}(k))\,\mathbf{m}^{(1)} = (\mathbf{\Omega}_{(2)}(k) - \overline{\mathbf{\Omega}}_{(2)}(k))\,\mathbf{m}^{(2)} \quad (22)$$

$$(\mathbf{\Omega}_{(1)}(k) - \overline{\mathbf{\Omega}}_{(1)}(k))\,\mathbf{m}^{(1)} = -i\frac{\Lambda}{1-k}[(\mathbf{M}_{(1)}^{-1}\,\mathbf{\Omega}_{(1)}(k) + \overline{\mathbf{M}}_{(1)}^{-1}\,\overline{\mathbf{\Omega}}_{(1)}(k))\,\mathbf{m}^{(1)} - (\mathbf{M}_{(2)}^{-1}\,\mathbf{\Omega}_{(2)}(k) + \overline{\mathbf{M}}_{(2)}^{-1}\,\overline{\mathbf{\Omega}}_{(2)}(k))\,\mathbf{m}^{(2)}] \quad (23)$$

where $\Lambda = [\lambda_{ij}]$ is the interfacial stiffness parameter matrix. Note that the condition $u_2^{(1)}(r, 0) > u_2^{(2)}(r, 0)$ is assumed for no material overlap at the interface. Equations (22) and (23) can written in matrix form as

$$\mathbf{K}^I(k)\,\mathbf{g} = \mathbf{0} \quad (24)$$

where the 6×6 matrix $\mathbf{K}^I(k)$ is given by

$$\mathbf{K}^I(k) = \begin{bmatrix} \mathbf{\Omega}_{(1)}(k) - \overline{\mathbf{\Omega}}_{(1)}(k) & -\mathbf{\Omega}_{(2)}(k) + \overline{\mathbf{\Omega}}_{(2)}(k) \\ i(1-k)(\mathbf{\Omega}_{(1)}(k) - \overline{\mathbf{\Omega}}_{(1)}(k)) - \mathbf{\Lambda}(\mathbf{M}_{(1)}^{-1}\mathbf{\Omega}_{(1)}(k) & + \overline{\mathbf{M}}_{(1)}^{-1}\,\overline{\mathbf{\Omega}}_{(1)}(k))\,\mathbf{\Lambda}(\mathbf{M}_{(2)}^{-1}\mathbf{\Omega}_{(2)}(k) + \overline{\mathbf{M}}_{(2)}^{-1}\,\overline{\mathbf{\Omega}}_{(2)}(k)) \end{bmatrix} \quad (25)$$

and $\mathbf{g} = \{m_1^{(1)}, m_2^{(1)}, m_3^{(1)}, m_1^{(2)}, m_2^{(2)}, m_3^{(2)}\}^T$. The order of singularity is determined by the condition that

$$|\,\mathbf{K}^I(k)\,| = 0 \quad (26)$$

For the contact conditions shown in Eq. (21), there are three displacement discontinuities in the x_1-, x_2-, x_3-directions at the interface. For the particular case where the displacements u_2 and u_3 are continuous while there is a displacement discontinuity in the x_1-direction only, the contact conditions can be written as,

$$t_i^{(1)}(r, 0) = t_i^{(2)}(r, 0) \qquad i = 1, 2, 3 \quad (27a)$$

$$u_i^{(1)}(r, 0) = u_i^{(2)}(r, 0)\,,$$

$$t_1^{(1)}(r, 0) = \frac{\lambda_{1j}}{r}[u_j^{(1)}(r, 0) - u_j^{(2)}(r, 0)] \qquad i = 2, 3 \quad (27b)$$

Equation (27a) is the continuity of traction given by Eq. (22), while Eq. (27b) can be written in matrix form as

$$\begin{Bmatrix} t_1(r,0) \\ 0 \\ 0 \end{Bmatrix} = \begin{bmatrix} \lambda_{11} & 0 & 0 \\ 0 & 1 & 0 \\ 0 & 0 & 1 \end{bmatrix} \begin{Bmatrix} u_1^{(1)}(r,0) - u_1^{(2)}(r,0) \\ u_2^{(1)}(r,0) - u_2^{(2)}(r,0) \\ u_3^{(1)}(r,0) - u_3^{(2)}(r,0) \end{Bmatrix} \tag{28}$$

Let **D** = diag(1, 0, 0) and **I** be the identity matrix, then Eq. (28) can be expressed as

$$\mathbf{D}\mathbf{t}^{(1)}(r,0) = (\mathbf{D}\boldsymbol{\Lambda}\mathbf{D} + \mathbf{I} - \mathbf{D})\,(\mathbf{u}^{(1)}(r,0) - \mathbf{u}^{(2)}(r,0)) \tag{29}$$

Substituting Eqs. (18a), (18b) and (19a) in Eq. (29) yields

$$\begin{aligned} &\mathbf{D}(\boldsymbol{\Omega}_{(1)}(k) - \overline{\boldsymbol{\Omega}}_{(1)}(k))\,\mathbf{m}^{(1)} \\ &\quad = -i\frac{\mathbf{Z}}{1-k}[(\mathbf{M}_{(1)}^{-1}\boldsymbol{\Omega}_{(1)}(k) + \overline{\mathbf{M}}_{(1)}^{-1}\overline{\boldsymbol{\Omega}}_{(1)}(k))\,\mathbf{m}^{(1)} \\ &\quad\quad - (\mathbf{M}_{(2)}^{-1}\boldsymbol{\Omega}_{(2)}(k) + \overline{\mathbf{M}}_{(2)}^{-1}\overline{\boldsymbol{\Omega}}_{(2)}(k))\,\mathbf{m}^{(2)}] \end{aligned} \tag{30}$$

where $\mathbf{Z} = \mathbf{D}\boldsymbol{\Lambda}\mathbf{D} + \mathbf{I} - \mathbf{D}$.

Now the order of singularity k can be determined from the characteristic equation

$$\begin{vmatrix} \boldsymbol{\Omega}_{(1)}(k) - \overline{\boldsymbol{\Omega}}_{(1)}(k) & -\boldsymbol{\Omega}_{(2)}(k) + \overline{\boldsymbol{\Omega}}_{(2)}(k) \\ i(1-k)\,\mathbf{D}\,(\boldsymbol{\Omega}_{(1)}(k) - \overline{\boldsymbol{\Omega}}_{(1)}(k)) - \mathbf{Z}(\mathbf{M}_{(1)}^{-1}\boldsymbol{\Omega}_{(1)}(k) + \overline{\mathbf{M}}_{(1)}^{-1}\overline{\boldsymbol{\Omega}}_{(1)}(k)) & \mathbf{Z}(\mathbf{M}_{(2)}^{-1}\boldsymbol{\Omega}_{(2)}(k) + \overline{\mathbf{M}}_{(2)}^{-1}\overline{\boldsymbol{\Omega}}_{(2)}(k)) \end{vmatrix} = 0 \tag{31}$$

or other displacement constraints given in Table 1 the stress singularity parameter k can also be calculated from Eq. (31).

Table 1 Matrix **D** for all possible displacement constraints

Displacement constraint	D
$u_1^{(1)}(r,0) = u_1^{(2)}(r,0)$	diag(0, 1, 1)
$u_2^{(1)}(r,0) = u_2^{(2)}(r,0)$	diag(1, 0, 1)
$u_3^{(1)}(r,0) = u_3^{(2)}(r,0)$	diag(1, 1, 0)
$u_i^{(1)}(r,0) = u_i^{(2)}(r,0),\quad i = 1, 2$	diag(0, 0, 1)
$u_i^{(1)}(r,0) = u_i^{(2)}(r,0),\quad i = 1, 3$	diag(0, 1, 0)
$u_i^{(1)}(r,0) = u_i^{(2)}(r,0),\quad i = 2, 3$	diag(1, 0, 0)
$u_i^{(1)}(r,0) = u_i^{(2)}(r,0),\quad i = 1, 2, 3$	diag(0, 0, 0)

For the general case where all displacements are discontinuous **D** = **I**. In addition the case of traction constraints $t_i^{(1)}(r,0) = t_i^{(2)}(r,0) = 0$, $i = 1, 2, 3$, then $\lambda_{ij} = 0$, $j = 1, 2, 3$.

5. NUMERICAL RESULTS

For numerical calculations the angle-ply bimaterial composite wedge is considered to consist of the same graphite/epoxy fiber-reinforced material with the elastic constants

$$\begin{aligned} &E_1 = 137.90\text{GPa}\ (20\times10^6\,\text{psi}) \\ &E_2 = E_3 = 14.48\text{GPa}\ (2.1\times10^6\,\text{psi}) \\ &G_{12} = G_{23} = G_{13} = 5.86\text{GPa}\ (0.85\times10^6\,\text{psi}) \\ &\nu_{12} = \nu_{23} = \nu_{13} = 0.21 \end{aligned} \tag{32}$$

where E_i, G_{ij} and ν_{ij} are the Young's modulus, shear modulus and Poisson's ratio, respectively (Wang and Crossman [18]). The ply angles of adjacent layers are $\phi^{(1)}$ and $\phi^{(2)}$ as shown in Fig. 2. To calculate p_α from Eq. (2a) it is necessary to determine C_{ijkl} which is related to the stiffness matrix C_{mn}. To determine C_{mn}, first the compliance matrix S_{mn}^* in local coordinates is calculated from the elastic constants given in Eq. (32), then the stiffness matrix C_{mn}^* in local coordinate is calculated by inverting S_{mn}^*, and finally the stiffness matrix C_{mn} of each layer is calculated from C_{mn}^* using a transformation formula. More details can be found in Poonsawat, *et al*. [8].

The three particular geometries considered are (a) the free-edge of a laminate, (b) the 90° broken laminate, and (c) the inclined broken laminate, as shown in Fig. 3. For the imperfect interface it is assumed that a displacement discontinuity is allowed only in the x_1-direction while the displacements in x_2- and x_3-directions are continuous, hence **D** = diag(1, 0, 0) and the relevant components of $\boldsymbol{\Lambda}$ are λ_{11}. For the fully bonded case and imperfect interface case the order of singularity k, where $0 < \text{Re}(k) < 1$ are calculated from Eq. (31). For all three configurations from geometrical considerations it is expected that the singularity is identical for the $(\phi^{(1)}/\phi^{(2)})$ and $(-\phi^{(1)}/-\phi^{(2)})$ composite wedges. In addition, since the singularity for the $(90°/\phi^{(2)})$ and $(-90°/\phi^{(2)})$ composite wedges are identical, the results presented in Tables 2 ~ 5 are for $-90° \le \phi^{(1)} \le 75°$ and $0° \le \phi^{(2)} \le 90°$.

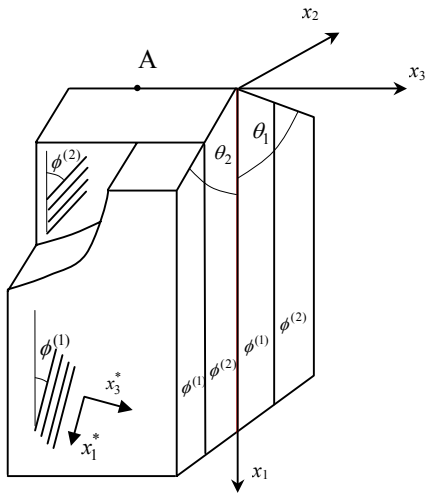

Fig. 2 An angle ply bimaterial wedge

Table 2 Angle-ply bimaterial wedge: free-edge of a graphite/epoxy laminate ($\theta_1 = \theta_2 = 90°$), variation of singularity with $\phi^{(1)}$ and $\phi^{(2)}$ for $\lambda_{11} = E_2$

$\phi^{(2)}$ \ $\phi^{(1)}$	– 90°	– 75°	– 60°	– 45°	– 30°	– 15°	0°	15°	30°	45°	60°	75°
0°	0.0613 –	0.0610 –	0.0584 –	0.0546 –	0.0613 –	0.1057 0.0010	0.1312 –	0.1057 0.0010	0.0613 –	0.0546 –	0.0584 –	0.0610 –
15°	0.0522 –	0.0527 –	0.0497 –	0.0419 –	0.0309 –	0.0597 0.0089	0.1057 0.0010	0.1016 –	0.0613 –	0.0495 –	0.0522 –	0.0535 –
30°	0.0318	0.0346	0.0353	0.0305	0.0234	0.0309	0.0613	0.0613	0.0103	0.0186	0.0297	0.0338
45°	0.0130	0.0165	0.0219	0.0256	0.0305	0.0419	0.0546	0.0495	0.0186	–	0.0068	0.0134
60°	0.0030	0.0050	0.0117	0.0219	0.0353	0.0497	0.0584	0.0522	0.0297	0.0068	–	0.0024
75°	0.0001	0.0006	0.0050	0.0165	0.0346	0.0527	0.0610	0.0535	0.0338	0.0134	0.0024	–
90°	–	0.0001	0.0030	0.0130	0.0318	0.0522	0.0613	0.0522	0.0318	0.0130	0.0030	0.0001

Table 3 Angle-ply bimaterial wedge: free-edge of a graphite/epoxy laminate ($\theta_1 = \theta_2 = 90°$), variation of singularity with $\phi^{(1)}$ and $\phi^{(2)}$ for a sliding interface

$\phi^{(2)}$ \ $\phi^{(1)}$	– 90°	– 75°	– 60°	– 45°	– 30°	– 15°	0°	15°	30°	45°	60°	75°
0°	–	0.0002	0.0024	0.0056	0.0056	0.0022	–	0.0022	0.0056	0.0056	0.0024	0.0002
15°	0.0018	0.0035	0.0098	0.0156	0.0152	0.0089	0.0022	–	0.0007	0.0005	–	0.0011
30°	0.0044	0.0076	0.0170	0.0243	0.0234	0.0152	0.0056	0.0007	–	–	0.0007	0.0037
45°	0.0045	0.0079	0.0180	0.0256	0.0243	0.0156	0.0056	0.0005	–	–	0.0008	0.0039
60°	0.0020	0.0041	0.0117	0.0180	0.0170	0.0098	0.0024	–	0.0007	0.0008	–	0.0014
75°	0.0001	0.0006	0.0041	0.0079	0.0076	0.0035	0.0002	0.0011	0.0037	0.0039	0.0014	–
90°	–	0.0001	0.0020	0.0045	0.0044	0.0018	–	0.0018	0.0044	0.0045	0.0020	0.0001

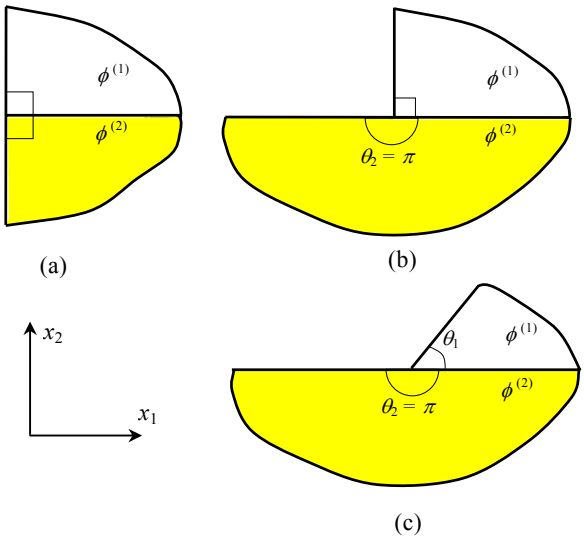

Fig. 3 Wedge configurations considered for numerical results (a) the free-edge of a laminate (b) the 90° broken laminate and (c) the inclined broken laminate

For the free-edge of a laminate the wedge angles $\theta_1 = \theta_2 = 90°$ (Fig. 3(a)). The order of singularity k for the fully bonded interface (i.e., when $\mathbf{D} = \mathbf{0}$) was obtained and agrees with the results of Zwiers, *et al*. [5] and Table 1 of Poonsawat, *et al*. [8], where it is found that for this particular bimaterial anisotropic wedge max(k) = 0.0334 when $(\phi^{(1)}/\phi^{(2)}) = (0°/90°)$. For the imperfect interface when $\lambda_{11} = E_2$, the order of singularity k is given in Table 2. Here it is seen that for different combinations of $(\phi^{(1)}/\phi^{(2)})$ that either there are no roots, one real root or two real root only and that max(k) = 0.1312 when $(\phi^{(1)}/\phi^{(2)}) = (0°/0°)$. For the fully sliding case when $\lambda_{11} = 0$, the order of singularity k is given in Table 3, where it is seen that for different combinations of $(\phi^{(1)}/\phi^{(2)})$ that either there are no roots or one real root only and that max(k) = 0.0256 when $(\phi^{(1)}/\phi^{(2)} = (-45°/45°)$. This max($k$) value is lower than that of the fully bonded case and much lower than that of the imperfect interface case. It is seen that for some combinations of $(\phi^{(1)}/\phi^{(2)})$ the order of singularity of the imperfect interface case is much more severe than that of both fully bonded and fully sliding interfaces. Due to geometrical considerations for any interfacial condition, k is identical for $(\phi^{(1)}/\phi^{(2)})$ and $(-\phi^{(2)}/-\phi^{(1)})$ composite wedges and this feature also has been noted by Poonsawat, *et al*. [8]. In addition when $\phi^{(1)} = \phi^{(2)}$ it is found that the power singularity does not occur for both fully bonded and fully sliding cases but may occur in the case of an imperfect interface.

For the 90° broken laminate the wedge angles $\theta_1 = 90°$ and $\theta_2 = 180°$ (Fig. 3(b)). The order of singularity k for the fully bonded interface (i.e., when $\mathbf{D} = \mathbf{0}$) was obtained and agrees with the results in Table 3 of Poonsawat, *et al*. [8], where it is found that three real roots occur in the range $0 < \mathrm{Re}(k) < 1$ and $\max(k) = 0.4930$ when $(\phi^{(1)}/\phi^{(2)}) = (0°/90°)$ and $\min(k) = 0.3962$ when $(\phi^{(1)}/\phi^{(2)}) = (-90°/0°)$. For $\lambda_{11} = E_2$, the order of singularity is shown in Table 4. It can be seen that in the range $0 < \mathrm{Re}(k) < 1$ three real roots of k exist and $\max(k) = 0.5324$ when $(\phi^{(1)}/\phi^{(2)}) = (0°/75°)$ or $(0°/90°)$ and $\min(k) = 0.4299$ when $(\phi^{(1)}/\phi^{(2)}) = (-90°/0°)$. For the fully sliding case, i.e., when $\lambda_{11} = 0$, as shown in Table 5 there are only two roots of k in the range $0 < \mathrm{Re}(k) < 1$ which can be either real or complex conjugate pairs and $\max(\mathrm{Re}(k)) = 0.3912$ when $(\phi^{(1)}/\phi^{(2)}) = (\pm 60°/90°)$ and $\min(\mathrm{Re}(k)) = 0.2687$ when $(\phi^{(1)}/\phi^{(2)}) = (-90°/60°)$. It can be seen that the order of singularity of the imperfect interface case is more severe than the fully bonded and fully sliding cases.

For the inclined broken laminate where $\theta_2 = 180°$ (Fig. 3(c)) the variation of k is investigated by varying the wedge angle θ_1, for the ply angle combinations $(\phi^{(1)}/\phi^{(2)}) = (0°/90°)$, $(30°/-60°)$, $(60°/-30°)$ and $(90°/0°)$ and for the stiffness parameter $\lambda_{11}/E_2 = \infty$ (fully bonded case), 10, 1, 0.1, 0.01 and 0. Figures 4 ~ 7 show $\mathrm{Re}(k)$ where the real parts of complex conjugate roots are shown in dashed lines. The $\mathrm{Re}(k)$ for the fully bonded case Figs. 4(a), 5(a), 6(a) and 7(a) agree with Fig. 5 of Poonsawat, *et al*. [8].

In Fig. 4, for $(\phi^{(1)}/\phi^{(2)}) = (0°/90°)$ and $\lambda_{11} \neq 0$ when θ_1 gradually increases from 0°. There are two real roots of k until $\theta_1 \approx 70°$ and for higher values of θ_1 either there are three real roots or one real root and a complex conjugate pair of roots. When $\theta_1 = 180°$, *i.e*., for an interface crack $\max(\mathrm{Re}(k)) = 0.5$, 0.503, 0.528, 0.745, 0.911 for $\lambda_{11}/E_2 = \infty$, 10, 1, 0.1 and 0.01, respectively, and this agrees with of Ting [19] and Suo [20] for the case of a fully bonded interface. For $\lambda_{11} = 0$ there are either one or two real roots of k and at $\theta_1 = 180°$, $\mathrm{Re}(k) = 0.5$.

Table 4 Angle-ply bimaterial wedge: 90° broken graphite/epoxy laminate ($\theta_1 = 90°$, $\theta_2 = 180°$), variation of singularity with $\phi^{(1)}$ and $\phi^{(2)}$ for $\lambda_{11} = E_2$

$\phi^{(2)}$ \ $\phi^{(1)}$	− 90°	− 75°	− 60°	− 45°	− 30°	− 15°	0°	15°	30°	45°	60°	75°
0°	0.4299 0.3333 0.0538	0.4315 0.3694 0.0547	0.4467 0.3874 0.0620	0.4723 0.3789 0.0798	0.4971 0.3620 0.1087	0.5164 0.3431 0.1412	0.5240 0.3333 0.1573	0.5164 0.3431 0.1412	0.4971 0.3620 0.1087	0.4723 0.3789 0.0798	0.4467 0.3874 0.0620	0.4315 0.3694 0.0547
15°	0.4366 0.3213 0.0567	0.4404 0.3556 0.0570	0.4585 0.3703 0.0627	0.4818 0.3618 0.0781	0.5026 0.3459 0.1039	0.5186 0.3288 0.1362	0.5255 0.3206 0.1593	0.5184 0.3344 0.1512	0.4973 0.3597 0.1203	0.4686 0.3809 0.0886	0.4434 0.3872 0.0676	0.4363 0.3595 0.0582
30°	0.4502 0.2955 0.0651	0.4537 0.3310 0.0651	0.4698 0.3491 0.0697	0.4907 0.3415 0.0836	0.5090 0.3249 0.1072	0.5224 0.3056 0.1379	0.5286 0.2931 0.1651	0.5235 0.3059 0.1642	0.5046 0.3361 0.1360	0.4770 0.3612 0.1030	0.4547 0.3653 0.0791	0.4497 0.3343 0.0674
45°	0.4635 0.2721 0.0783	0.4659 0.3095 0.0782	0.4790 0.3322 0.0824	0.4977 0.3263 0.0961	0.5141 0.3088 0.1184	0.5258 0.2872 0.1470	0.5312 0.2700 0.1744	0.5278 0.2787 0.1762	0.5133 0.3094 0.1501	0.4901 0.3358 0.1185	0.4696 0.3408 0.0938	0.4633 0.3108 0.0810
60°	0.4729 0.2664 0.0920	0.4746 0.3051 0.0922	0.4853 0.3304 0.0977	0.5024 0.3251 0.1130	0.5176 0.3062 0.1359	0.5279 0.2830 0.1628	0.5323 0.2658 0.1853	0.5296 0.2757 0.1816	0.5184 0.3041 0.1564	0.4998 0.3286 0.1279	0.4812 0.3341 0.1057	0.4734 0.3055 0.0942
75°	0.4773 0.2944 0.0991	0.4785 0.3330 0.1000	0.4880 0.3574 0.1079	0.5043 0.3509 0.1260	0.5192 0.3305 0.1512	0.5288 0.3071 0.1771	0.5324 0.2943 0.1915	0.5294 0.3065 0.1809	0.5196 0.3312 0.1557	0.5039 0.3528 0.1293	0.4870 0.3591 0.1097	0.4782 0.3334 0.1005
90°	0.4779 0.3333 0.0999	0.4790 0.3695 0.1010	0.4882 0.3905 0.1097	0.5044 0.3833 0.1290	0.5192 0.3644 0.1553	0.5290 0.3435 0.1806	0.5324 0.3333 0.1922	0.5290 0.3435 0.1806	0.5192 0.3644 0.1553	0.5044 0.3833 0.1290	0.4882 0.3905 0.1097	0.4790 0.3695 0.1010

Table 5 Angle-ply bimaterial wedge: 90° broken graphite/epoxy laminate ($\theta_1 = 90°$, $\theta_2 = 180°$), variation of singularity with $\phi^{(1)}$ and $\phi^{(2)}$ for a sliding interface

$\phi^{(2)}$ \ $\phi^{(1)}$	− 90°	− 75°	− 60°	− 45°	− 30°	− 15°	0°	15°	30°	45°	60°	75°
0°	0.3333 0.2070	0.3695 0.2076	0.3910 0.2127	0.3838 0.2233	0.3638 0.2363	0.3431 0.2482	0.3333 0.2539	0.3431 0.2482	0.3638 0.2363	0.3838 0.2233	0.3910 0.2127	0.3695 0.2076
15°	0.3253 0.2090	0.3619 0.2098	0.3832 0.2154	0.3750 0.2264	0.3545 0.2394	0.3338 0.2513	0.3249 0.2563	0.3366 0.2490	0.3587 0.2364	0.3790 0.2238	0.3856 0.2139	0.3625 0.2094
30°	0.3042 0.2144	0.3419 0.2153	0.3638 0.2213	0.3548 0.2324	0.3331 0.2456	0.3108 0.2585	0.3018 0.2636	0.3181 0.2523	0.3425 0.2385	0.3635 0.2264	0.3692 0.2178	0.3433 0.2143
45°	0.2791 0.2210	0.3177 0.2218	0.3408 0.2277	0.3317 0.2384	0.3094 0.2513	0.2806 0.2702	0.2735 $\pm 0.0109i$	0.2981 0.2541	0.3237 0.2397	0.3442 0.2292	0.3486 0.2223	0.3199 0.2202
60°	0.2687 0.2250	0.3077 0.2257	0.3324 0.2307	0.3250 0.2397	0.3044 0.2504	0.2797 0.2649	0.2703 $\pm 0.0092i$	0.2921 0.2535	0.3155 0.2414	0.3347 0.2324	0.3385 0.2264	0.3094 0.2244
75°	0.2946 0.2262	0.3333 0.2269	0.3578 0.2315	0.3508 0.2405	0.3302 0.2519	0.3075 0.2644	0.2943 0.2732	0.3096 0.2626	0.3327 0.2499	0.3530 0.2389	0.3592 0.2305	0.3336 0.2266
90°	0.3333 0.2264	0.3696 0.2271	0.3912 0.2321	0.3841 0.2423	0.3644 0.2550	0.3435 0.2670	0.3333 0.2732	0.3435 0.2670	0.3644 0.2550	0.3841 0.2423	0.3912 0.2321	0.3696 0.2271

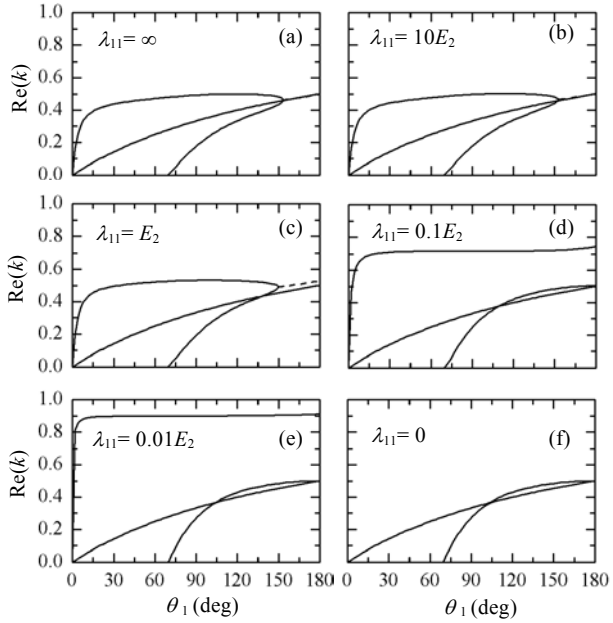

Fig. 4 Order of singularlity k for an inclined broken laminate for $(\phi^{(1)}/\phi^{(2)}) = (0°/90°)$; (—) k is real, (----) k is complex

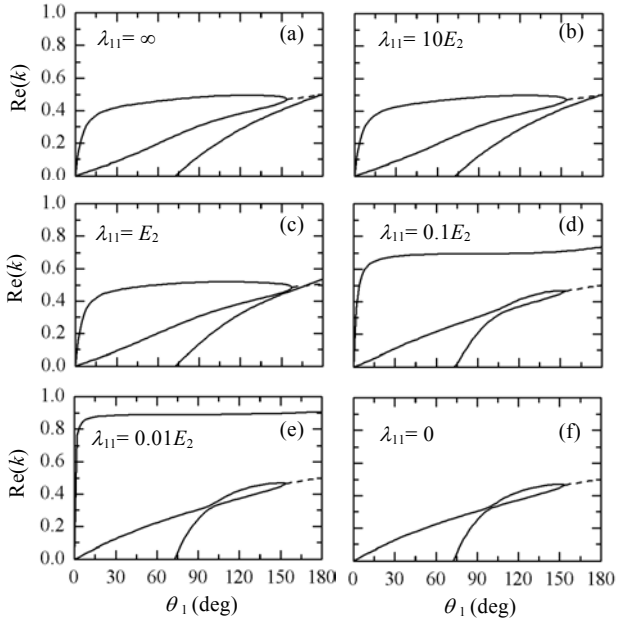

Fig. 5 Order of singularlity k for an inclined broken laminate for $(\phi^{(1)}/\phi^{(2)}) = (30°/–60°)$; (—) k is real, (----) k is complex

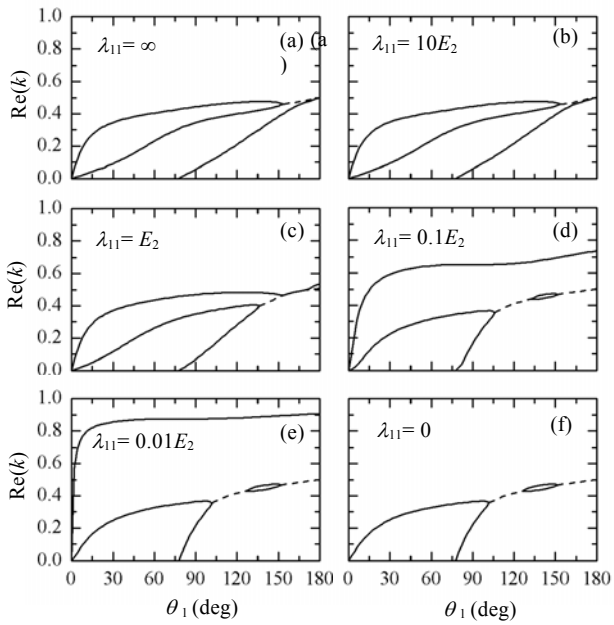

Fig. 6 Order of singularlity k for an inclined broken laminate for $(\phi^{(1)}/\phi^{(2)}) = (60°/–30°)$; (—) k is real, (----) k is complex

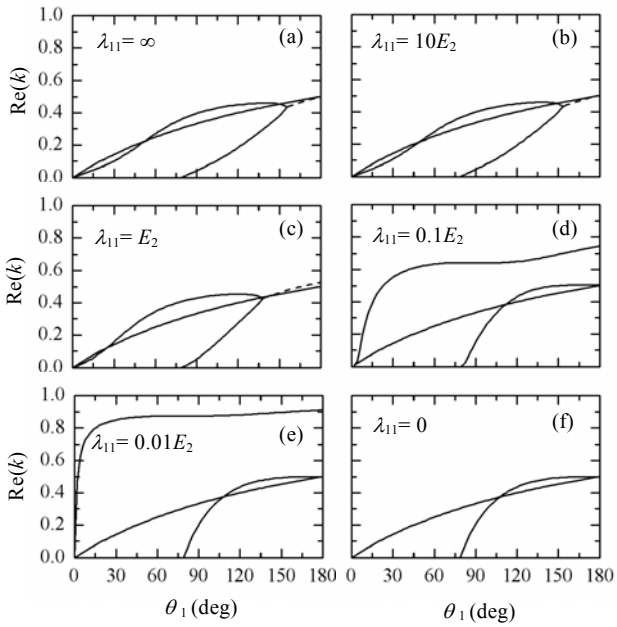

Fig. 7 Order of singularlity k for an inclined broken laminate for $(\phi^{(1)}/\phi^{(2)}) = (90°/0°)$; (—) k is real, (----) k is complex

The behavior of the order of singularity for the (90°/0°) composite wedge shown in Fig. 7 is similar to the (0°/90°) case shown in Fig. 4 and when $\theta_1 = 180°$ the max(Re(k)) of the (90°/0°) composite wedge is identical to the (0°/90°) case. From Figs. 4 and 7 it is seen that for the (0°/90°) and (90°/0°) composite wedges that there exists one real root of k which is identical for all values of λ_{11}. This identical root corresponds to the antiplane problem, because for (0°/0°) and (90°/?°) wedges the problems associated with inplane and antiplane deformations are uncoupled.

For the (30°/–60°) and (60°/–30°) composite wedges the order of singularity k is shown in Figs. 5 and 6. When θ_1 gradually increase from 0°, the behavior of the roots for the two cases are different, although when $\theta_1 = 180°$ for both wedges max(Re(k)) = 0.5, 0.503, 0.537, 0.737 and 0.906 for $\lambda_{11}/E_2 = \infty$, 10, 1, 0.1 and 0.01, respectively. Here too, for the fully bonded case the results agree with Ting [19] and Suo [20]. For $\lambda_{11} = 0$ there are either one real root, two real roots or a pair of complex conjugate roots and at $\theta_1 = 180°$, Re(k) = 0.5.

6. SUMMARY AND CONCLUSIONS

The characteristic equation to obtain the order of stress singularity for bimaterial anisotropic composite wedges with an imperfect interface subjected to traction free boundary conditions is presented. The imperfect interface feature model is such that the interfacial tractions are continuous, directly proportional to the displacement discontinuities and inversely proportional to the radial coordinate. The numerical results obtained for an angle-ply bimaterial wedge agree with available results for the fully bonded case.

ACKNOWLEDGEMENT

The authors wish to acknowledge that their work in the area of anisotropic elastic media have been very much influenced by the monograph and research papers of Prof. T. C. T. Ting.

REFERENCES

1. Benthem, J. P., "On the Stress Distribution in Anisotropic Wedges," *Quarterly of Applied Mathematics*, 21, pp. 189–198 (1963).
2. Ma, C.-C. and Hour, B.-L., "Analysis of Dissimilar Anisotropic Wedges Subjected to Antiplane Shear Deformation," *International Journal of Solids and Structures*, 25, pp. 1295–1309 (1989).
3. Chue, C.-H. and Liu, C.-I., "A General Solution on Stress Singularities in an Anisotropic Wedge," *International Journal of Solids and Structures*, 38, pp. 6889–6906 (2001).
4. Wang, S. S. and Choi, I., "Boundary-Layer Effects in Composite Laminates; Part I, Free-Edge Stress Singularities; Part II, Free-Edge Stress Solutions and Characteristics," *ASME Journal of Applied Mechanics*, 49, pp. 541–550 (1982).
5. Zwiers, R. I., Ting, T. C. T. and Spilker, R. L., "On the Logarithmic Singularity of Free-Edge Stress in Laminated Composites Under Uniform Extension," *ASME Journal of Applied Mechanics*, 49, pp. 562–569 (1982).
6. Delale, F., "Stress Singularities in Bonded Anisotropic Materials," *International Journal of Solids and Structures*, 20, pp. 31–41 (1984).
7. Lin, Y. Y. and Sung, J. C., "Stress Singularities at the Apex of a Dissimilar Anisotropic Wedge," *ASME Journal of Applied Mechanics*, 65, pp. 454–463 (1998).
8. Poonsawat, P., Wijeyewickrema, A. C., Karasudhi, P., "Singular Stress Fields of Angle-ply and Monoclinic Bimaterial Wedges," *International Journal of Solids and Structures*, 38, pp. 91–113 (2001).
9. Chue, C.-H., Chen, T.-H. and Lee, H.-T., "A General Solution in Stress Singularities in the Junction of Two Anisotropic Materials," *Composite Structures*, 55, pp. 81–93 (2002).
10. Chue, C.-H. and Liu, C.-I., "Disappearance of Free-Edge Stress Singularity in Composite Laminates," *Composite Structures*, 56, pp. 111–129 (2002).
11. Chue, C.-H. and Liu, C.-I., "Stress Singularities in Bimaterial Anisotropic Wedge with Arbitrary Fiber Orientation," *Composite Structures*, 58, pp. 49–56 (2002).
12. Mishuris, G. S., "Influence of Interfacial Models on a Stress Field Near a Crack Terminating at a Bimaterial Interface," *International Journal of Solids and Structures*, 34, pp. 37–46 (1997).
13. Mishuris, G. S., "Asymptotics of the Elastic Solution of a Plane Problem Near the Crack Tip Terminating at a Nonideal Bimaterial Interface (Mode I and II)," *Mechanics of Composite Materials*, 34, pp. 439–456 (1998).
14. Mishuris, G. S., "Stress Singularity at a Crack Tip for Various Intermediate Zones in Bimaterial Structures (Mode III)," *International Journal of Solids and Structures*, 36, pp. 999–1015 (1999).
15. Stroh, A. N., "Dislocations and Cracks in Anisotropic Elasticity," *Philosophical Magazine*, 3, pp. 625–646 (1958).
16. Eshelby, J. D., Read, W. T. and Shockley, W., "Anisotropic Elasticity with Applications to Dislocation Theory," *Acta Metallurgica*, 1, pp. 251–259 (1953).
17. Ting, T. C. T. and Chou, S. C., "Edge Singularities in Anisotropic Composites," *International Journal of Solids and Structures*, 17, pp. 1057–1068 (1981).
18. Wang, A. S. D. and Crossman, F. W., "Some New Results on Edge Effects in Symmetric Composite Laminates," *Journal of Composite Materials*, 11, pp. 92–106 (1977).
19. Ting, T. C. T., "Explicit Solution and Invariance of the Singularities at an Interface Crack in Anisotropic Composites," *International Journal of Solids and Structures*, 22, pp. 965–983 (1986).
20. Suo, Z., "Singularities, Interfaces and Cracks in Dissimilar Anisotropic Media" *Proceedings of the Royal Society of London*, 331–358, p. A427 (1990).